Hybrid nonlocality via atom photon interactions with and without impurities

Pritam Halder¹, Ratul Banerjee¹, Saptarshi Roy², Aditi Sen(De)¹

¹ Harish-Chandra Research Institute, A CI of Homi Bhabha National Institute, Chhatnag Road, Jhunsi, Allahabad - 211019, India

² QICI Quantum Information and Computation Initiative, Department of Computer Science,

The University of Hong Kong, Pokfulam Road, Hong Kong

To obtain Bell statistics from hybrid states composed of finite- and infinite-dimensional systems, we propose a hybrid measurement scheme, in which the continuous mode is measured using the generalized pseudospin operators, while the finite (two)-dimensional system is measured in the usual Pauli basis. Maximizing the Bell expression with these measurements leads to the violations of local realism which is referred to as *hybrid non-locality*. We demonstrate the utility of our strategy in a realistic setting of cavity quantum electrodynamics, where an atom interacts with a single mode of an electromagnetic field under the Jaynes-Cummings Hamiltonian. We dynamically compute the quenched averaged value of hybrid nonlocality in imperfect situations by incorporating disorder in the atom-cavity coupling strength. In the disordered case, we introduce two kinds of measurement scenarios to determine the Bell statistics – in one situation, experimentalists can tune the optimal settings according to the interaction strength while such controlled power is absent in the other case. In contrast to the oscillatory behavior observed in the ordered case, the quenched averaged violation saturates to a finite value in some parameter regimes in the former case, thereby highlighting an advantage of disordered systems. We also examine the connection between Wigner negativity and hybrid nonlocality.

I. INTRODUCTION

John S. Bell discovered a set of mathematical inequalities [1] to determine whether a theory can be compatible with the assumptions of locality and reality [2]. It was shown that there exist quantum states which violate Bell's inequalities, thereby revealing the incompatibility with Einstein, Podolski and Rosen's argument of local realism [2]. This nonclassical feature of quantum mechanics is, in fact, one of the foundational pillars to *understand* the quantum world. It has also been experimentally demonstrated multiple times over the past fifty years that states having quantum correlations aka entanglement, violate Bell inequalities [3–6]. Apart from fundamental implications on the structure of the theory, violation of Bell inequalities also certifies supremacy in a number of tasks like device-independent quantum key distribution [7, 8], random number generation [9], self-testing [10] etc., as a resource quantifier [11, 12] for developing quantum technologies.

It has recently been realized that the development of modern quantum architectures requires cross-platform information processing where different nodes of the network comprise different types of systems, commonly referred to as hybrid systems [13] consisting of discrete and continuous variable (CV) counterparts [13, 14]. The majority of theoretical and experimental research of hybrid systems to date have centred on characteristics like nonclassicality [15], and entanglement [16–18]. It is important here to emphasize that investigating violations of Bell inequality differs qualitatively from studying correlations like entanglement since the statistics required to construct the Bell expression depend on the choice of measurements. For example, even the singlet state may fail to show any violation if the appropriate measurements are not chosen to extract the Bell statistics. Our aim in this work is to construct a suitable framework for testing the violation of local realism in hybrid systems, thereby, illustrating the interplay between hybrid states and measurements.

In discrete systems, violations of Bell inequalities are rou-

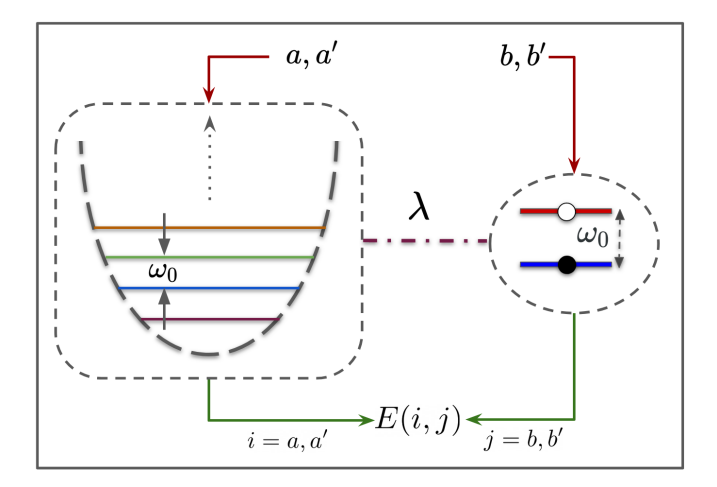


FIG. 1. (Color online.) Schematic diagram of the extraction of Bell statistics via correlation functions, E(i,j), from a hybrid system with i=a,a' and j=b,b' being the measurement settings at sites A and B of the entire system. The hybrid system consists of an atom (subsystem A) and a single mode of a quantized electromagnetic field (modelled as a cavity), referred to as subsystem B, which interacts via Jaynes-Cummings Hamiltonian. ω_0 is the resonant frequency which corresponds to both the frequency of the cavity and the energy gap of the atom. The atom-photon interaction follows a coupling strength λ .

tinely investigated both theoretically and experimentally, although, for CV systems, the Bell expression to examine the violation of local realism is not straightforward. Specifically, J.S. Bell [1] himself argued that Gaussian states which possess positive (Gaussian) Wigner functions, would not violate these inequalities. This was believed to be true for a long time until it was disproved by employing [19, 20] non-Gaussian measurements to extract the violation out of Gaussian states. In particular, the maximal violation for the Einstein Podolski Rosen (EPR) state [2] is obtained using pseudospin operators [20] (later generalized pseudospin operators [21]). Neverthe-

less, the connection of negativity in Wigner function with its maximal violation of Bell inequality by a quantum state is an interesting question and has been pursued in several works for CV systems [19, 20, 22]. We intend to investigate the link, if any, between these two quantities for hybrid quantum systems

To investigate the violation of Bell inequality for a prototypical hybrid system consisting of an atom (a qubit) and a single mode of light (CV system) (see Fig. 1), we integrate the concepts both from qubit and CV systems. Specifically, to acquire the Bell statistics, we introduce a hybrid measurement strategy that uses Pauli measurement on an atom and generalized pseudospin operators in the CV component of the system [20, 21].

In this work, initial states are taken to be either a product or classically correlated or entangled in the atom-light bipartition which are allowed to interact via the Jaynes-Cummings Hamiltonian [23, 24]. In the case of separable states, the CV system is either in the Fock or squeezed or coherent state. On the other hand, the hybrid cat state [18] is chosen to be the initial state which is, in general, entangled. We find that the maximal violation of Bell inequality oscillates with time and is highly dependent on the parameters involved in CV systems. We establish a connection between the violation of local realism, initial entanglement and hybrid Wigner negativity volume [18, 25].

Departing from the ideal situation, we introduce impurities in the interaction strength. We demonstrate that the quenched averaged violation persists even in the presence of disorder, the oscillations observed in the ordered system vanish and saturate to some nonvanishing value when it is assumed that experimentalists are permitted to adjust the measurement settings in each realization of disorder. On the other hand, if the measurements are fixed to be optimal for the mean value of the random Gaussian disorder, we report that a violation of local realism is obtained only for a certain period of time, after which no violation is detected.

The paper is organized as follows. We introduce the formalism to evaluate hybrid nonlocality using hybrid measurements in Sec. II. The details of setting up the optimization problem are discussed in Sec. II A, while the Wigner negativity volume is defined in Sec. II B. The generation and dynamics of hybrid nonlocality via atom-photon interactions are illustrated in Sec. III. We provide a brief primer on the atom-photon interactions via the Jaynes-Cummings Hamiltonian in Sec. III A, and examples of different initial states, separable in Sec. III B and entangled in Sec. III C. The violation obtained in the dynamical states is compared with their Wigner negativity volume in Sec. IV. Finally, we study the effects of imperfections on the Bell-violation in Sec. V, where we investigate the role of disorder in the coupling strength of the atom-photon interactions. A conclusion is provided in Sec. VI.

II. HYBRID NONLOCALITY USING HYBRID MEASUREMENTS

Let us start our discussion with a particular variant of Bell inequalities, namely the Clauser-Horn-Shimony-Holt (CHSH) inequalities [26, 27]. It turns out to be the facet (tight) ones in the 2-2-2-configuration (2 parties, 2 measurement settings, 2 outcomes per measurement) [28].

Let us explain the CHSH inequality briefly which gives us the premise to detect quantum correlations in hybrid systems. Consider an arbitrary two-party state, ρ , shared between A and B in spatially separated locations. For each party, two different dichotomic measurements, a, a' and b, b' are employed. Depending on the settings, the measurement outcomes are denoted by A_i and B_j with i = a, a' and j = b, b' for A and B respectively. The assumptions of locality and realism lead to the upper bound 2 of the Bell expression, given by

$$\mathcal{B} = |E(a,b) + E(a',b) + E(a,b') - E(a',b')|, \quad (1)$$

where the correlation function $E(i,j) = \langle A_i B_j \rangle_{\rho}$. The maximal violation that can be achieved via a quantum state is given by the Tsirelson's bound [29] for which $|\mathcal{B}^Q|_{\max} = 2\sqrt{2}$.

The statistics of the Bell CHSH expression are generated by the outcomes of dichotomic measurements on quantum states ρ . For continuous variable systems, the choice of these two outcome measurements that results in maximal violation, in principle, requires a search over an infinite number of parameters. This, in general, makes the problem of choosing optimal measurements very hard [19] for CV systems. Let us first discuss a type of dichotomic continuous variable pseudospin measurements that were introduced [20] to extract maximal violation of the CHSH inequality for two-mode squeezed vacuum states. Specifically, we consider a more generalized version, called the generalized pseudospin operators [20–22],

$$S_q^z = \sum_{\substack{n=0\\2n+q>0}}^{\infty} |2n+q+1\rangle\langle 2n+q+1| - |2n+q\rangle\langle 2n+q|,$$

$$S_q^- = \sum_{\substack{n=0\\2n+q \ge 0}}^{\infty} |2n+q\rangle\langle 2n+q+1| = (S_q^+)^{\dagger}, \tag{2}$$

where q is an integer.

A. Constructing Bell inequalities using hybrid measurement strategies

We are now positioned to formulate the Bell CHSH expression of a hybrid quantum system. While the party with the qubit system performs the usual Pauli measurements, the party which possesses the infinite dimensional system employs the pseudospin measurements to extract the required statistics for constructing the Bell expression. The correlation functions of a given state, ρ , that constitute the Bell expression can be written as

$$E(i,j) = \text{Tr}[S_i^q \otimes \sigma_i \rho], \tag{3}$$

where $\sigma_j=\cos\theta_j\sigma_z+\sin\theta_j(e^{i\phi_j}\sigma_++e^{-i\phi_j}\sigma_-)$, and $S_i^q=\cos\theta_iS_z^q+\sin\theta_i(e^{i\phi_i}S_+^q+e^{-i\phi_i}S_-^q)$. The Pauli ladder operators can be written in terms of Pauli spin operators as $\sigma_\pm=(\sigma_x\pm i\sigma_y)/2$. Similarly, like the usual Pauli operators, S_x^q and S_y^q are given by $S_+^q+S_-^q$ and $-i(S_+^q-S_-^q)$ respectively, where S_+^q and S_-^q are given in Eq. (2). The measurements are parameterized by their respective polar $(0\leq\theta_k\leq\pi)$ and azimuthal $(0\leq\phi_l\leq2\pi)$ angles. We are interested in the maximal violation of Bell inequality by a given quantum state which we obtain by optimizing over the measurement parameters as

$$|\mathcal{B}|_{\max} = \max_{\boldsymbol{\theta}, \boldsymbol{\Phi}, a} |\mathcal{B}|,\tag{4}$$

where $\boldsymbol{\theta} = (\theta_a, \theta_{a'}, \theta_b, \theta_{b'})$ and $\boldsymbol{\Phi} = (\phi_a, \phi_{a'}, \phi_b, \phi_{b'})$.

1. Maximization of Bell expression

We now present a brief primer on how to obtain $|\mathcal{B}|_{\max}$ by performing maximization over the settings, i.e., θ , Φ and q. The elements of the correlation matrix, T, in the hybrid systems is defined by $T_{kl} = \langle S_k^q \otimes \sigma_l \rangle$, where k, l = x, y, z. The value of q is chosen depending on the structure of the shared state. Following the prescribed strategy [30], the maximal violation of Bell inequality can again be expressed as $2\sqrt{\Lambda_1 + \Lambda_2}$, where Λ_1 and Λ_2 denote the two largest eigenvalues of $T^\dagger T$. Although this nine parameter problem is hard to track analytically, we can reduce the number of parameters to be optimized for some cases and can obtain an analytical closed form expression of the optimal Bell-CHSH violation.

B. Wigner negativity volume

Introduced by Wigner in 1932 [31], Wigner functions have been rigorously used in quantum optics as a detector of non-classicality [25]. The Wigner function is defined in the phase space as the Fourier transform of the symmetrized characteristic function [32]. For a single mode CV system, ρ , the Wigner function can be expressed as [24]

$$W(x,p) = \frac{1}{2\pi} \int_{-\infty}^{+\infty} \left\langle x + \frac{1}{2}q \middle| \rho \middle| x - \frac{1}{2}q \right\rangle e^{ipq} dq, \quad (5)$$

where $\left|x\pm\frac{1}{2}q\right\rangle$ denote the eigenstates of the X-quadrature. Although it satisfies the normalization condition, i.e., $\int W(x,p)dxdp=1$, it is interpreted as a quasi probability distribution since the Wigner function may not always be positive throughout the phase space. The negativity of the Wigner function (W(x,p)<0) for some states, in turn, aids to gauge its nonclassicality. The nonclassicality detection capabilities of the Wigner function can be turned into a measure, when one considers the volume of Wigner function in the phase space where it is negative. Technically, it is called the Wigner negativity volume [25], and is defined as

$$\mathcal{V}_n = \int_{W(x,p)<0} W(x,p) dx dp. \tag{6}$$

We now briefly describe the prescription for the computation of Wigner negativity volume for hybrid quantum systems [18]. The Wigner function of a hybrid quantum state ρ consisting of both discrete and continuous variables is given by [33]

$$W(\theta, \phi, \beta) = \text{Tr} \left[\rho \, \hat{\Delta}_c(\beta) \otimes \hat{\Delta}_d(\theta, \phi) \right], \tag{7}$$

where

$$\hat{\Delta}_c(\beta) = \frac{2}{\pi} \hat{D} \hat{\Pi}_c \hat{D}^{\dagger}, \text{ and } \hat{\Delta}_d(\theta, \phi) = \frac{1}{2} \hat{U} \hat{\Pi}_q \hat{U}^{\dagger}, \quad (8)$$

stand for kernel operators corresponding to the CV and qubit systems, respectively. Here, $\hat{D}(\beta) = e^{\hat{a}^\dagger \beta - \hat{a} \beta^*}$ is the displacement operator and $\hat{\Pi}_c = e^{i\pi\hat{a}^\dagger\hat{a}}$ is the parity operator for the CV system. In the qubit scenario, $\hat{U} \in SU(2)$, which can be written in terms of Pauli operators $\sigma_i, i=1,2,3$ as $\hat{U}=e^{i\sigma_3\phi}e^{i\sigma_2\theta}e^{i\sigma_3\Phi}$, where $\theta\in[0,\pi]$ and $\phi,\Phi\in[0,2\pi]$ and the parity operator for qubit is given by $\hat{\Pi}_d=\mathbb{I}-\sqrt{3}\sigma_3$.

The normalization condition for the hybrid Wigner function is obtained from the Haar measure [34], $d\Omega$, such that $\int W d\Omega = 1$. The integral measure $d\Omega$ is a product of the Haar measure for qubits $(d\nu)$ which turns out to be the differential volume of the SU(2) space corresponding to a qubit and the differential volume of the field of coherent states $d^2\beta$. The integral measure, therefore, becomes

$$d\Omega = d\nu d^2\beta = \frac{1}{\pi}\sin 2\theta d\theta d\phi d^2\beta,\tag{9}$$

with $\theta \in [0, \pi/2]$ and $\phi \in [0, 2\pi]$. We then compute the hybrid Wigner negative volume (\mathcal{V}_n) by

$$\mathcal{V}_n = \frac{1}{2} \int (|W| - W) d\Omega = \frac{1}{2} \left(\int |W| d\Omega - 1 \right). \tag{10}$$

In this work, we intend to investigate whether there exists some connection between the maximal violation of hybrid Bell inequality, $|\mathcal{B}|_{\text{max}}$ and Wigner negativity volume, \mathcal{V}_n .

III. GENERATION AND DYNAMICS OF HYBRID NONLOCALITY

We explore how atom-photon interactions can generate hybrid correlations from an initially separable state, which can lead to the violation of the Bell-CHSH inequality based on pseudospin operator formalism as laid out in Sec. II A. Further, starting from a hybrid entangled initial state that violates the Bell inequality, we also track how the dynamics generated by the atom-photon interactions can sustain, enhance or deteriorate the initial violation. Before moving on to explicit examples, we first present a brief description of the atom-photon interaction that is considered in this manuscript.

A. Modelling atom-photon interactions: Jaynes-Cummings Hamiltonian

Interaction between quantized electromagnetic field and atomic system that can be modelled via the prototypical Jaynes-Cummings (JC) Hamiltonian. Here the light and matter are both taken as quantum,i.e., a quantized electromagnetic field and a two level system respectively. Recently, it has been possible to create environments capable of supporting a single mode field, such as small microwave cavities, optical cavities etc [35–38]. In our case, we will concentrate on a setup where a single mode light field interacts with a two level system. The atomic transition and inversion operators obeying Pauli spin algebra are respectively given by

$$\sigma_{+} = |e\rangle \langle g|, \ \sigma_{-} = |g\rangle \langle e|, \ \text{and} \ \sigma_{z} = |e\rangle \langle e| - |g\rangle \langle g(11)$$

For all these operators, we have $[\sigma_+, \sigma_-] = \sigma_z$, $[\sigma_z, \sigma_{\pm}] = \pm 2\sigma_{\pm}$. The total atom-field Hamiltonian can be written as

$$H = H_A + H_F + H_I$$

= $\frac{1}{2}\hbar\omega_0\sigma_z + \hbar\omega a^{\dagger}a + \hbar\lambda(a + a^{\dagger})(\hat{\sigma}_+ + \sigma_-).$ (12)

Here H_A is the atomic Hamiltonian with energy gap $\hbar\omega_0$ between the energy levels (\hbar is Planck's constant), H_F describes the free electromagnetic field with frequency ω and H_I characterizes the interaction between atom and field with interaction strength λ . Note that the terms $a^\dagger\sigma_+$ and $a\sigma_-$ correspond to the energy non-conserving terms which vary rapidly in time, are dropped using rotating wave approximation (RWA). Finally, we can write the JC Hamiltonian as

$$H = \frac{1}{2}\hbar\omega_0\sigma_z + \hbar\omega\hat{a}^{\dagger}a + \hbar\lambda(a\sigma_+ + a^{\dagger}\sigma_-).$$
 (13)

In our work, we take the detuning parameter $\delta=\omega-\omega_0=0$, i.e., the resonance condition, $\omega=\omega_0$. Therefore, our JC Hamlitonian becomes

$$H = H_0 + H_I, \tag{14}$$

where

$$H_0 = \frac{1}{2}\hbar\omega_0\sigma_z + \hbar\omega_0a^{\dagger}a,$$
 and $H_I = \hbar\lambda(a\sigma_+ + a^{\dagger}\sigma_-).$ (15)

In the interaction picture, the time evolution unitary of Eq. (14) can be written as

$$U_{\lambda}(t) = e^{-iH_{I}t/\hbar} = e^{-i\lambda t(a\sigma_{+} + a^{\dagger}\sigma_{-})}$$

$$= \cos\left(\sqrt{a^{\dagger}a}\lambda t\right)|e\rangle\langle e| - ia\frac{\sin\left(\sqrt{a^{\dagger}a}\lambda t\right)}{\sqrt{a^{\dagger}a}}|e\rangle\langle g|$$

$$- ia^{\dagger}\frac{\sin\left(\sqrt{aa^{\dagger}}\lambda t\right)}{\sqrt{aa^{\dagger}}}|g\rangle\langle e| + \cos\left(\sqrt{a^{\dagger}a}\lambda t\right)|g\rangle\langle g|.$$
(16)

The above unitary operator will be used to obtain dynamical state whose nonlocal features will be studied.

B. Generation of hybrid nonlocality for different initial separable states

Let us analyze how nonlocality can be generated with time via atom-photon interactions from initial separable hybrid states. Let us take the initial state as any general single qubit and a single mode continuous variable state in the eigenbasis of their respective local Hamiltonians. It can be expressed as

$$|\psi(0)\rangle_{\text{atom}} = C_g |g\rangle + C_e |e\rangle$$
, and $|\psi(0)\rangle_{\text{field}} = \sum_{n=0}^{\infty} C_n |n\rangle$. (17)

Clearly, $|g(e)\rangle$ denotes the ground (excited) state of H_A wheras $\{|n\rangle\}$ constitute the Fock basis. Therefore, any separable hybrid state can be written as a convex combination of states written as a tensor product of qubit and CV states of the form given in Eq. (17).

1. Initial product hybrid states

The initial hybrid state in product form can, in general, be written as $|\psi(0)\rangle = |\psi(0)\rangle_{\text{field}} \otimes |\psi(0)\rangle_{\text{atom}}$. As the initial state is product in field-atom bipartition, following unitary with the JC interaction, the time evolved hybrid state can be written as

$$|\psi(t)\rangle = U_I(t) |\psi(0)\rangle$$

$$= \sum_{n=0}^{\infty} \left\{ \left[C_e C_n \cos \left(\lambda t \sqrt{n+1} \right) - i C_g C_{n+1} \sin \left(\lambda t \sqrt{n+1} \right) \right] | e \right\}$$

$$+\left[-iC_{e}C_{n-1}\sin\left(\lambda t\sqrt{n}\right) + C_{g}C_{n}\cos\left(\lambda t\sqrt{n}\right)\right]\left|g\right\rangle\right\}\left|n\right\rangle.$$
 (18)

Let us assume that the atom is initially in the excited state, i.e., $C_e = 1$, $C_g = 0$ and we write Eq. (18) as

$$|\psi(t)\rangle = |\psi_a(t)\rangle |g\rangle + |\psi_e(t)\rangle |e\rangle,$$
 (19)

where

$$|\psi_g(t)\rangle = -i\sum_{n=0}^{\infty} C_n \sin(\lambda t \sqrt{n+1}) |n+1\rangle,$$
and $|\psi_e(t)\rangle = \sum_{n=0}^{\infty} C_n \cos(\lambda t \sqrt{n+1}) |n\rangle.$ (20)

The correlation matrix T_{ij} as described in Sec. II A 1 for the states of the form in Eq. (19) can be computed as

$$T_{ij} = \langle \psi(t) | S_i^q \otimes \sigma_j | \psi(t) \rangle$$

$$= \langle \psi_g(t) | S_i^q | \psi_g(t) \rangle \langle g | \sigma_j | g \rangle + \langle \psi_e(t) | S_i^q | \psi_e(t) \rangle \langle e | \sigma_j | e \rangle$$

$$+ \langle \psi_g(t) | S_i^q | \psi_e(t) \rangle \langle g | \sigma_j | e \rangle + \langle \psi_e(t) | S_i^q | \psi_g(t) \rangle \langle e | \sigma_j | g \rangle.$$
(21)

We now compute the maximal violation of the Bell-CHSH inequality, $|\mathcal{B}|_{\max}$ by taking different initial states, i.e., different C_n 's at any instant of time.

a. kth Fock basis as the initial field state. If the electromagnetic field is initally in the kth Fock basis, i.e.,

$$C_n = \delta_{n,k},\tag{22}$$

the time evolved hybrid state reads as

$$|\psi(t)\rangle = \cos\left(\lambda t \sqrt{k+1}\right) |k\rangle |e\rangle$$

- $i \sin\left(\lambda t \sqrt{k+1}\right) |k+1\rangle |g\rangle$, (23)

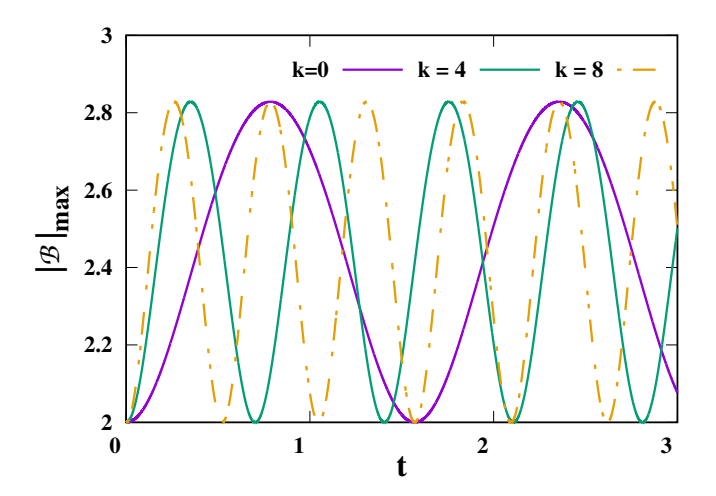


FIG. 2. (Color online.) Dynamics of $|\mathcal{B}|_{\max}$ (ordinate) with time, t (abscissa). The initial state is taken to be the kth Fock state in the CV part. We choose different values of k=0,4, and 8, which illustrate different oscillation periods of $|\mathcal{B}|_{\max}$. Both axes are dimensionless.

which leads to the maximal violation at any instant of time as

$$|\mathcal{B}|_{\text{max}} = 2\sqrt{1 + \sin^2\left(2\lambda\sqrt{1 + kt}\right)}.$$
 (24)

We find that the state becomes entangled for all k and the entire range of t values except for a few distinct values, $|\mathcal{B}|_{\max} > 2$ as also shown in Fig. 2. Depending on k, only the period of oscillation changes as seen from Eq. (24).

b. Initial field prepared in SMSV state. Let us move to the scenario where the initial CV system is in a single-mode squeezed vacuum (SMSV) state having the form

$$|\psi(0)\rangle_{\text{field}} = S(\xi)|0\rangle = |\xi\rangle = \sum_{n=0}^{\infty} C_n|n\rangle,$$
 (25)

with
$$C_n = \begin{cases} (-1)^{n/2} \frac{\sqrt{n!}}{2^{\frac{n}{2}} \frac{n}{2}!} \frac{(e^{i\theta} \tanh(r))^{\frac{n}{2}}}{\sqrt{\cosh(r)}} & \text{if n is even ,} \\ 0 & \text{if n is odd,} \end{cases}$$
 (26)

where
$$S(\xi)=\exp\left[\frac{1}{2}(\xi^*a^2-\xi a^{\dagger 2})\right], \qquad \xi=re^{i\theta}.$$
 (27)

Following the prescription, described in Sec. II A, we find the maximal Bell violation for each q denoted by $|\mathcal{B}|_{\max}^q$ where optimizations over θ , Φ are already performed. For q=0,

the correlation matrix takes the form as
$$T = \begin{pmatrix} 0 & \epsilon & 0 \\ -\epsilon & 0 & 0 \\ 0 & 0 & -1 \end{pmatrix}$$
 and the corresponding $|\mathcal{B}|^0 = 2\sqrt{1+\epsilon^2}$ with the dis

and the corresponding $|\mathcal{B}|_{\max}^0 = 2\sqrt{1+\epsilon^2}$ with the directions being derived as $\theta = (\pi, \frac{\pi}{2}, \tan^{-1}\epsilon, -\tan^{-1}\epsilon)$ and $\Phi = (\phi, 0, \frac{\pi}{2}, \frac{\pi}{2}), \ 0 \leq \phi \leq 2\pi$ which implies that the maximization is independent of ϕ . In case of q=

1,
$$T = \begin{pmatrix} \kappa_1 & \kappa_2 & 0 \\ \kappa_2 & -\kappa_1 & 0 \\ 0 & 0 & \kappa_3 \end{pmatrix}$$
. If $\kappa_3^2 > \kappa_1^2 + \kappa_2^2$, we obtain $\kappa_3^2 > \kappa_1^2 + \kappa_2^2$, we obtain $\kappa_3^2 > \kappa_1^2 + \kappa_2^2$.

tain $|\mathcal{B}|_{\max}^1 = 2\sqrt{\kappa_3^2 + (\kappa_1^2 + \kappa_2^2)}$ and optimizing directions

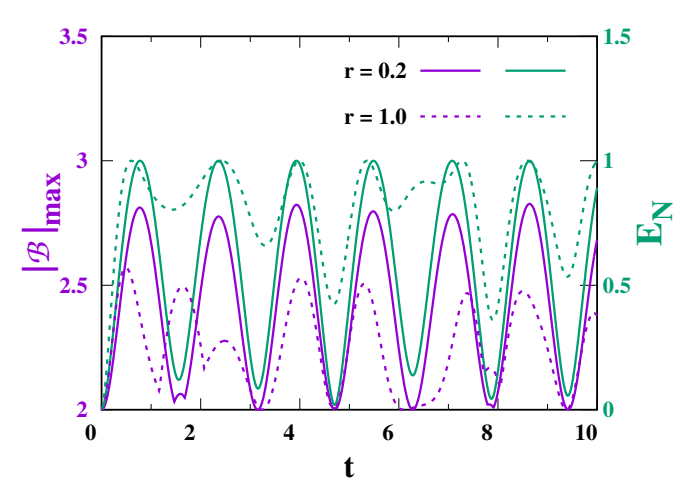


FIG. 3. (Color online.) Dynamics of maximal violation of Bell inequality, $|\mathcal{B}|_{\max}$ (left ordinate) with time t (abscissa) of the time evolved hybrid state, where the initial state in the CV sector is a single mode squeezed vacuum (SMSV) state with the atom initially being in the excited state. We consider two different values of squeezing strength, r=0.2, and 1.0. We plot the entanglement content, E_N (right ordinate), quantified by the von Neumann entropy of the local density matrix of the time evolved state against time which connects E_N with $|\mathcal{B}|_{\max}$. Both axes are dimensionless.

are $\boldsymbol{\theta}=(0,\frac{\pi}{2},\tan^{-1}\sqrt{\kappa_1^2+\kappa_2^2},-\tan^{-1}\sqrt{\kappa_1^2+\kappa_2^2})$, $\boldsymbol{\Phi}=(\phi,\tan^{-1}(-\frac{\kappa_1}{\kappa_2}),\frac{\pi}{2},\frac{\pi}{2})$. Finally, for $\kappa_3^2<\kappa_1^2+\kappa_2^2$, the maximal Bell violation reads as $|\mathcal{B}|_{\max}^1=2\sqrt{2}\sqrt{\kappa_1^2+\kappa_2^2}$ along with the optimal measurement directions being calculated as $\boldsymbol{\theta}=(\frac{\pi}{2},\frac{\pi}{2},\frac{\pi}{2},\frac{\pi}{2})$ and $\boldsymbol{\Phi}=(\tan^{-1}\frac{\kappa_2}{\kappa_1},\tan^{-1}(-\frac{\kappa_1}{\kappa_2}),\frac{\pi}{4},\frac{7\pi}{4})$. Thus depending on the above conditions, we get $|\mathcal{B}|_{\max}=\max\{|\mathcal{B}|_{\max}^0,|\mathcal{B}|_{\max}^1\}$ where the range of q from which the maximal violation obtained, is confirmed via numerical investigation.

In Fig. 3, we show the time dynamics of the maximal Bell expression and show that during the entire evolution $|\mathcal{B}|_{\max} \geq 2$. We also compare the dynamical violation with the entanglement content of the state. Since the time evolved state is pure, the entanglement can simply be quantified by the entanglement entropy, i.e., the von Neumann entropy of the reduced density matrix given by $E_N = \mathcal{S}(\rho_d(t)) = -\text{Tr}[\rho_d(t)\log_2\rho_d(t)]$ with $\rho_d(t)$ being the reduced density matrix of the qubit subsystem of the time evolved state. Moreover, with the increase of squeezing strength, the maximal value, $|\mathcal{B}|_{\max}$, for a fixed time interval depicts an overall declining feature, although the fall is not always monotonic. Interestingly, if we keep on increasing r, we observe that after a certain critical value $r = r_c$ of the field, the maximal violation for the hybrid system completely vanishes.

c. Coherent state as initial field state. Let us choose the displaced vacuum in the Fock basis,

$$|\psi(0)\rangle_{\text{field}} = D(\alpha)|0\rangle = |\alpha\rangle$$
 (28)

where $|\alpha\rangle = \sum_{n=0}^{\infty} C_n |n\rangle$, with $C_n = \frac{e^{-|\alpha^2|}\alpha^n}{\sqrt{n!}}$, $\alpha = |\alpha|e^{i\theta}$ as the initial field state. In this case, the number of optimizing parameters cannot be reduced like in the previous sce-

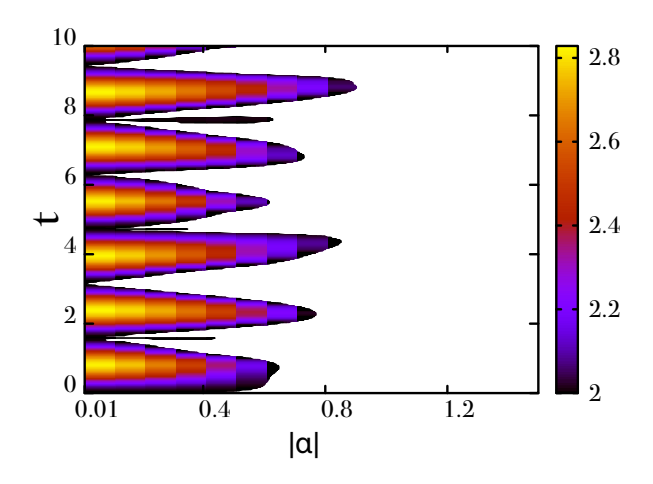


FIG. 4. (Color online.) A heat map plot of $|\mathcal{B}|_{\max}$ in the $(|\alpha|,t)$ -(horizontal-vertical axis) plane where the initial CV system is taken as a coherent state which evolves under JC Hamiltonian. The uncoloured (white) regions denote the non-violating zones. Both axes are dimensionless.

nario. Therefore, we perform the optimization using numerical techniques where we find the maximal violation by directly finding the eigenvalues of the correlation matrix using standard numerical eigensolvers. Moreover, we scan the space of $q \in \mathbb{N}$ and find the value of q that optimizes the Bell expression to be between 0 to 5. For a particular time interval, optimizing over the measurement settings, θ, Φ, q , and by varying the displacement strength $|\alpha|$ of the coherent state, $|\mathcal{B}_{\max}|$, shows an oscillatory behaviour (see Fig. 4).

Despite being entangled at certain times, it does not violate Bell inequality at those times due to the fact that the pseudospin operators do not form a basis for all dichotomic operators in space of single mode continuous variable state in the first party. For a particular time interval, the total time span at which we are detecting the Bell nonlocality through hybrid spin formalism decreases with the increase of displacement of the coherent state since it fails to completely capture the full two-party correlation, as shown in Fig. 5. Furthermore, we notice that there is a critical value of $|\alpha|$ beyond which the state does not violate the Bell inequality (see Fig. 4).

2. Classically correlated states as inputs

Instead of product states, let us allow the initial hybrid state to share some classical correlation which can be prepared via local operation and classical communication (LOCC). For example, we take

$$\rho(0) = p |e, \alpha\rangle \langle e, \alpha| + (1 - p) |q, -\alpha\rangle \langle q, -\alpha|. \tag{29}$$

Here we take three different values of p=0.2,0.5 and 0.8. For p=0.2, the state is a convex mixture of two different separable states which is close to a pure state $|g,-\alpha\rangle$. For p=0.5, it is an equal mixture and p=0.8, the classically correlated state has less distance with a pure state, $|e,\alpha\rangle$.

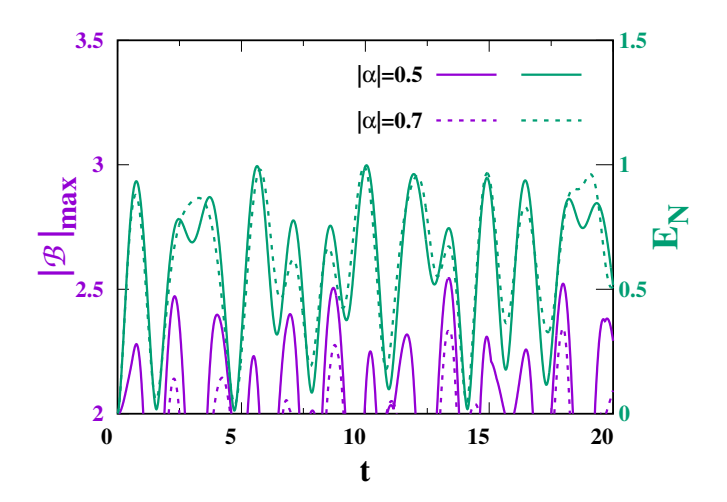


FIG. 5. (Color online.) Connecting entanglement (right ordinate) with the maximal violation of Bell inequality (left ordinate) for initial coherent states with two prototypical intensities: $|\alpha|=0.5$ and $|\alpha|=0.7$. A similar analysis for an initial SMSV state is demonstrated in Fig. 3. Both axes are dimensionless.

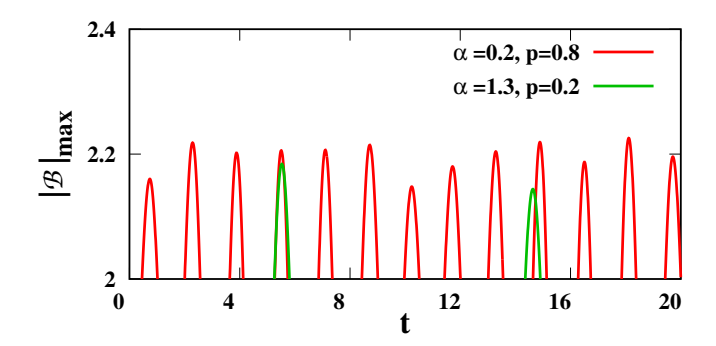


FIG. 6. (Color online.) For initial classically correlated states, $|\mathcal{B}|_{\max}$ (vertical axis) vs t (horizontal axis). We observe that only for low α - high p, and high α - low p values, there is a possibility for obtaining a finite violation of local realism. Both axes are dimensionless.

After the evolution of the initial state governed by Jaynes-Cummings Hamiltonian, we numerically compute the maximal Bell-CHSH expression at each time using Horodecki's criterion [30].

Depending on the displacement strength $|\alpha|$ of the initial CV system, we have different time dynamics of this maximal Bell expression. As shown in Fig. 6, with low displacement $|\alpha|=0.2$, and high p=0.8, we get a $|\mathcal{B}|_{\max}$ which crosses LHV bound 2 during the dynamics. For p=0.5 the same $|\alpha|$ value does not lead to a violation. Reversely, with high displacement $|\alpha|=1.3$, $|\mathcal{B}|_{\max}>2$ for p=0.2 while with p=0.5 and 0.8, $|\mathcal{B}|_{\max}<2$. In summary, violation of local realism with spin-pseudospin measurement is achieved for low p and high $|\alpha|$ or with high p and low $|\alpha|$. This is a prototypical example to show the efficacy of our method to detect the violation of local realism with mixed hybrid state having classical correlation.

So we can conclude that detecting violation of local realism

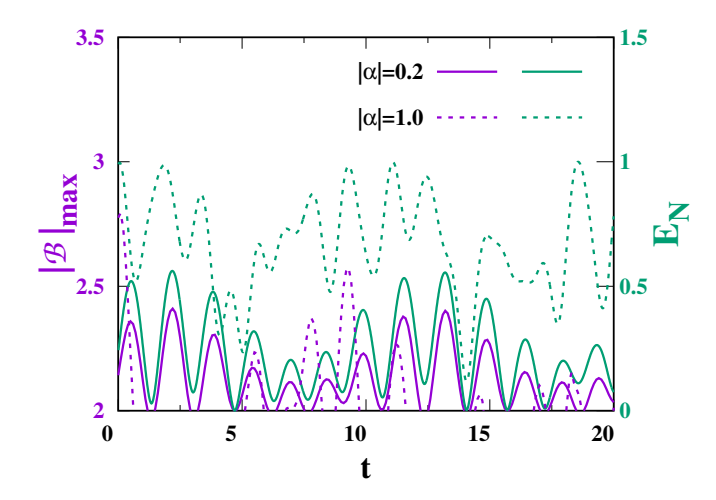


FIG. 7. (Color online.) Dynamics of the maximal violation of local realism $|\mathcal{B}|_{\max}$ (left ordinate) with time t (abscissa) of the hybrid cat state for different values of initial displacement $|\alpha|=0.2$, and, 1.0. For comparison, entanglement, E_N (right ordinate), of the same time evolved cat state is shown. Both axes are dimensionless.

in the context of spin-pseudospin measurement, is more successful for low p and high $|\alpha|$ or with high p and low $|\alpha|$. This is a prototypical example to show the efficacy of our method to detect the violation of Bell inequality in the mixed hybrid state regime too.

C. Dynamics of hybrid nonlocality for initially entangled states

We now change the gear by choosing the initial state as an entangled state, instead of the initial separable states studied before. Let us consider the cat state [24],

$$|\psi(0)\rangle = a_1 |\alpha\rangle |e\rangle + a_2 |-\alpha\rangle |g\rangle,$$
 (30)

as the initial state having bipartite entanglement. In Schrodinger picture, the evolved state reads as $|\psi(t)\rangle=e^{-iH_0t}U_I(t)\,|\psi(0)\rangle=|\psi_q(t)\rangle\,|g\rangle+|\psi_e(t)\rangle\,|e\rangle,$

where
$$|\psi_g(t)\rangle = \Big[\sum_{n=0}^{\infty} e^{-i\omega(n-1/2)t} \{-iC_{n-1}p_1\sin(\lambda t\sqrt{n}) + (-1)^n p_2 C_n\cos(\lambda t\sqrt{n})\} |n\rangle \Big],$$

and $|\psi_e(t)\rangle = \Big[\sum_{n=0}^{\infty} e^{-i\omega(n+1/2)t} \{C_n p_1\cos(\lambda t\sqrt{n+1}) - i(-1)^{n+1} p_2 C_{n+1}\sin(\lambda t\sqrt{n+1})\} |n\rangle \Big],$

$$(31)$$

with
$$C_n = \frac{e^{-|\alpha^2|}\alpha^n}{\sqrt{n!}}$$
. (32)

Note that irrespective of the value of frequency ω of JC Hamiltonian, we get the same $|\mathcal{B}|_{\text{max}}$ at all times with $a_1 = a_2 = \frac{1}{\sqrt{2}}$ which is due to the structure of the time evolved state.

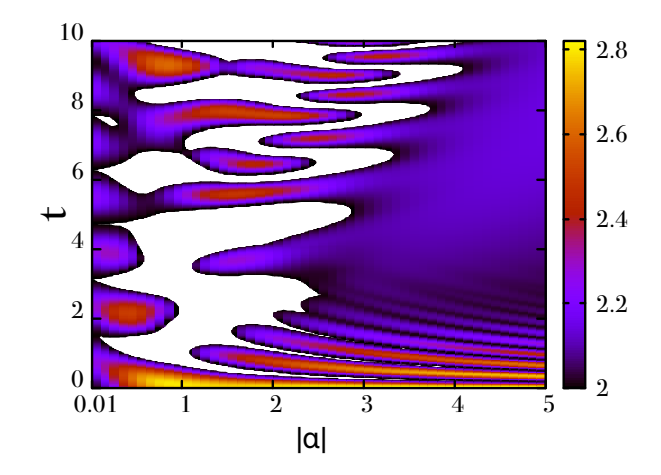


FIG. 8. (Color online.) Map plot of the maximal violation of Bell inequality in the $(|\alpha|,t)$ -plane for an initial cat state. The uncoloured (white) regions represent the non-violating river. By comparing with Fig. 4, we notice that for initial product state, no violation is observed for high $|\alpha|$ values $\forall t$ while in case of initial entangled state, the dynamical state always violates local realism, irrespective of $|\alpha|$ and t values. Both axes are dimensionless.

Firstly, the qubit subsystem can be written as

$$\rho_{q}(t) = |\psi_{g}(t)|^{2} |g\rangle \langle g| + |\psi_{e}(t)|^{2} |e\rangle \langle e| + \langle \psi_{e}(t)|\psi_{g}(t)\rangle |g\rangle \langle e| + \langle \psi_{g}(t)|\psi_{e}(t)\rangle |e\rangle \langle g|,$$
(33)

where

$$\langle \psi_g(t)|\psi_e(t)\rangle = \sum_{n=0}^{\infty} e^{-i\omega t} \{iC_{n-1}^* p_1 \sin(\lambda t \sqrt{n}) + (-1)^n p_2 C_n^* \cos(\lambda t \sqrt{n})\}$$
$$\times \{C_n p_1 \cos(\lambda t \sqrt{n+1}) - i(-1)^{n+1} p_2 C_{n+1} \sin(\lambda t \sqrt{n+1})\}.$$
(34)

When we derive the eigenvalues of ρ_d , we find that the phase factors with ω cancel out, which implies that the entanglement of the cat state is independent of the resonant frequency. Therefore, the entanglement of $|\psi(t)\rangle$ reduces to $E_N = \mathcal{S}(\rho_d(t))$. Fig. 7 again confirms that the trends of the overall dynamics of entanglement and the maximal violation of Bell inequality qualitatively match. In this situation also, we find that with increasing $|\alpha|$, the capability of capturing nonlocal correlation decreases by hybrid spin formalism. Moreover, from Fig. 8, it is evident that at time t=0with increasing $|\alpha|$, the maximal violation of Bell inequality rapidly increases, when $|\alpha|$ is small and then after showing a small dip, it saturates to $2\sqrt{2}$ for a certain range of displacement strength. Interestingly, from Fig. 8, we observe that for low values of $|\alpha|$, which corresponds to lower values of initial entanglement, a river of non-violating regime in the $(|\alpha|, t)$ plane emerges where no violation of Bell-CHSH inequality is found. However, when the initial entanglement is high indicated by higher $|\alpha|$ values, we obtain violation for all times.

IV. BASED ON PARITY OPERATOR, CONNECTING HYBRID WIGNER NON-CLASSICALITY WITH VIOLATION OF LOCAL REALISM

Investigation of the connection between negativity of the Wigner function dates back to the time of J. S. Bell who argued that Gaussian states would not violate a Bell inequality since they possess a Gaussian (positive) Wigner function [1]. However, Banaszek et. al. [19] conclusively showed that two-mode Gaussian states can violate Bell inequalities, thereby demonstrating a weak connection between the sign of the Wigner function of two-mode CV state and local realism. We intend to explore the possibility of establishing a connection between the hybrid versions of these quantities for bipartite states constituting of both discrete and continuous variable systems.

By considering all the initial product states and cat states, we evaluate \mathcal{V}_n defined in Eq. (10) and compare it with maximal violation of Bell inequality. The dynamical behaviour is similar for all initial states. For prototypical demonstration, we chose the initial state to be the cat state. Notice that unlike product states, this cat state violates local realism even at the initial time.

By substituting $a_1 = a_2 = \frac{1}{\sqrt{2}}$ in Eq. (30), the time evolved cat state can be written as

$$|\psi(t)\rangle_{\mathcal{C}} = \sum_{m=0}^{\infty} C_m^g(t) |m\rangle |g\rangle + \sum_{m=0}^{\infty} C_m^e(t) |m\rangle |e\rangle.$$
 (35)

The dynamical hybrid Wigner function for the time-evolved cat state can be written from Eq. (7) as

$$W(\theta, \phi, \beta) = \langle \psi(t) | \hat{\Delta}_c(\beta) \otimes \hat{\Delta}_d(\theta, \phi) | \psi(t) \rangle, \quad (36)$$

where $\hat{\Delta}_c(\beta)$ and $\hat{\Delta}_d(\theta,\phi)$ denote the kernel operators corresponding to the continuous and qubit systems respectively. It reduces to

$$W(\theta, \phi, \beta) = \sum_{n,m=0}^{\infty} C_n^{g*}(t) C_m^g(t) \langle n | \hat{\Delta}_c(\beta) | m \rangle$$

$$\times \left(\langle g | \hat{\Delta}_d(\theta, \phi) | g \rangle + \langle g | \hat{\Delta}_d(\theta, \phi) | e \rangle + \langle e | \hat{\Delta}_d(\theta, \phi) | g \rangle + \langle e | \hat{\Delta}_d(\theta, \phi) | e \rangle \right). (37)$$

By evaluating,

$$\langle n | \hat{\Delta}_c | m \rangle = \frac{2}{\pi} \sum_{n'=0}^{\infty} (-1)^{n'} \langle n | \hat{D}(\beta) | n' \rangle \langle n' | \hat{D}^{\dagger}(\beta) | m \rangle$$
$$= \frac{2}{\pi} F(n, m, \beta), \tag{38}$$

where

$$\langle k|\hat{D}(\beta)|l\rangle = \langle k|\beta,l\rangle$$

$$= \begin{cases} \langle 0|\beta\rangle \sqrt{\frac{l!}{k!}}\beta^{k-l}L_l^{k-l}(|\beta|^2), & k>l\\ \langle 0|\beta\rangle \sqrt{\frac{k!}{l!}}(-\beta^*)^{l-k}L_k^{l-k}(|\beta|^2), & l>k \end{cases}$$
(39)

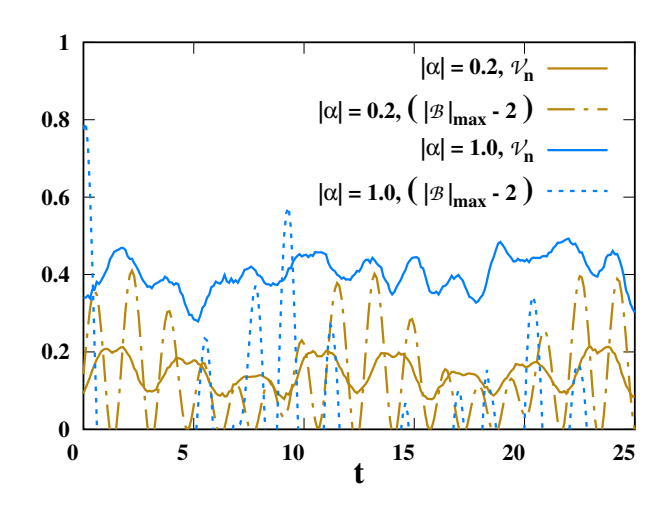


FIG. 9. (Color online.) Connection between the maximal violation of local realism, $|\mathcal{B}|_{\max} - 2$ (vertical axis) (dashed lines), and negative Wigner volume \mathcal{V}_n (vertical axis) indicated by solid lines, with time, t (horizontal axis) by taking the initial CV system to be in a cat state. Both axes are dimensionless.

with $\langle \beta | \alpha \rangle = e^{-\frac{1}{2}(|\alpha|^2+|\beta|^2+\alpha\beta^*)}$ and $L^n_m(x)$ is the Laguerre polynomial $L^n_m(x) = \sum_{i=0}^m \binom{m+n}{m-n} \frac{(-x)^i}{i!}$. Finally, we obtain

$$\begin{split} W(\theta,\phi,\beta) &= \frac{1}{\pi} \sum_{n,m=0}^{\infty} \{ (1+\sqrt{3}\cos 2\theta) C_n^{g*}(t) C_m^g(t) \\ &+ (1-\sqrt{3}\cos 2\theta) C_n^{e*}(t) C_m^e(t) \\ &+ (\sqrt{3}\sin 2\theta e^{i2\phi}) C_n^{e*}(t) C_m^g(t) \\ &+ (\sqrt{3}\sin 2\theta e^{-i2\phi}) C_n^{g*}(t) C_m^e(t) \} F(n,m,\beta). \end{split}$$

By integrating the negative part of the Wigner function over the Haar measure $d\Omega$ as defined in Eq. (9), we find the hybrid Wigner negativity, V_n in Eq. (10).

Our investigation clearly reveals that there is no one to one connection between the maximal violation of Bell inequalities and the negative Wigner volume in hybrid systems (see Fig.9) as also shown for CV systems [19].

V. EFFECT OF DISORDER IN ATOM-PHOTON INTERACTIONS

Till now, we have considered an idealized situation in which the quantum states are free from any noise and the time dynamics do not have any imperfection or disorder. However, in a realistic situation, imperfections are ubiquitous at all stages of quantum technology. This makes the investigation of imperfections and their corresponding robustness analysis absolutely crucial. In our work, we consider the situation where the coupling strength of the atom-photon interaction has some impurity. Such a situation might arise when the cavity is not fabricated perfectly resulting in varied imperfections like the

field inside the cavity not being uniform or the disorder being present in the coupling strength. We now examine whether the maximal violation of Bell inequality is robust against these imperfections.

Relevant physical quantities which is $|\mathcal{B}|_{\text{max}}$ in this case of such disordered systems are obtained by averaging over various realizations of the disorder, namely quenched averaging. It is performed when the equilibration time of the disorder which in the Javnes-Cummings interaction strength, λ is much longer compared to the observation time scales of the physical properties of the system. See previous work [39] in this respect. Therefore, one may consider the value of the impurities in the system to be effectively fixed during the dynamics of the system, thereby making it possible to carry out an averaging of the quantity of interest, Q, over the distribution of different values of the disordered parameters. Such a disordered system is realizable in current experimental setups using systems like cold atoms and trapped ions [40–43]. For randomly chosen interactions λ from a probability distribution $P(\lambda)$, the quench-averaged Q, denoted by $\langle Q \rangle$, at every time instant is given by

$$\langle \mathcal{Q} \rangle = \int \mathcal{Q}(\lambda) P(\lambda) d\lambda.$$
 (40)

Note that $P(x)=\delta(x-\lambda)$ corresponds to the disorder free case, which were discussed in the previous sections. To capture the effect of disorder, various forms of $P(\lambda)$ are chosen in the literature. The typical choices include uniform distribution, Gaussian distribution, Cauchy-Lorentz distribution [44–48] . In our work, we choose the values of λ from a Gaussian distribution with mean $\bar{\lambda}$ and standard deviation σ_{λ} , which can be called the strength of the disorder. Unlike entanglement measures [49], two different situations can be considered in this set up since one requires measurement outcomes to obtain Bell statistics.

A. Oracle measurement strategy

Depending on the value of the interaction strength in each realization λ , the state evolved through Jaynes-Cummings Hamiltonian and its time dependent correlation matrix can be written respectively as

$$\begin{split} T_{\lambda}^{ij}(t) &= \text{Tr}(\rho_{\lambda}(t)S_{i}^{q} \otimes \sigma_{j}), \\ \text{and } \rho_{\lambda}(t) &= U_{\lambda}(t)\rho_{in}U_{\lambda}^{\dagger}(t). \end{split} \tag{41}$$

Let us now suppose that the experimentalist has the ability to tune its measurement directions to reach the maximal Bell violation at any given time t depending on the particular realization λ . Hence, for every realization λ and at any given time instance t, we can apply the optimization strategy as laid out in Sec. II A 1 and we obtain

$$Q^{O}(\lambda) = |\mathcal{B}_{\rho_{\lambda}}|_{\max} = 2\sqrt{\Lambda_1 + \Lambda_2}, \tag{42}$$

where Λ_1 and Λ_2 denote the two largest eigenvalues of $T_{\lambda}^{\dagger}T_{\lambda}$, and O in the superscript denotes the oracle measurement strategy. Note that we drop the time index since it is fixed to a

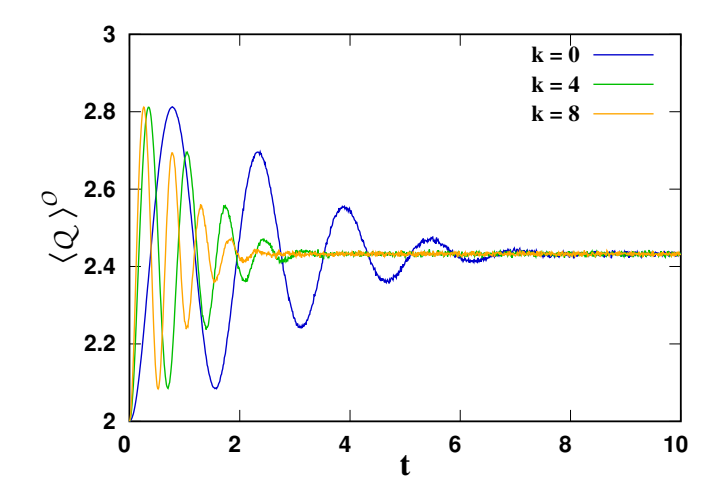


FIG. 10. (Color online.) The quenched averaged value of the maximal violation of local realism, $\langle \mathcal{Q} \rangle^O$ (vertical axis) for different values of k=0,4 and 8 against time, t (horizontal axis), where k denotes initial kth Fock state in the CV sector. Here, $\bar{\lambda}=1.0$, $\sigma_{\lambda}=0.1$. Saturation value of $\langle \mathcal{Q}^O \rangle_{\text{sat}}$ is ≈ 2.43 , and is independent of k. Both axes are dimensionless.

given point t. Nevertheless, for the disordered case, when the measurement settings can be chosen depending on a given realization λ , we are now equipped to calculate the quenched averaged maximal violation by using Eq. (40) as

$$\langle \mathcal{Q} \rangle^O = \int \mathcal{Q}^O(\lambda) P(\lambda) d\lambda.$$
 (43)

In this work, we consider the exemplary case where the disorder follows a Gaussian distribution,

$$P(\lambda) = \frac{1}{\sigma_{\lambda}\sqrt{2\pi}} \exp\frac{(\lambda - \bar{\lambda})^2}{2\sigma_{\lambda}^2},\tag{44}$$

where $\bar{\lambda}$ is the mean and the corresponding standard deviation is σ_{λ} . Here $\sigma_{\lambda}=0$ corresponds to the ordered case discussed in previous sections. We now present some examples to demonstrate how the disorder effects the violation of the Bell-CHSH inequality.

The first example we choose is when the initial state is a product state where the state of the field mode is in the k^{th} Fock basis (see Eq. (22)) and the atom is in the excited state. The maximal violation of local realism for any realization λ at any time slice t is given in Eq. (24). Therefore we have, $Q(\lambda) = 2\sqrt{1 + \sin^2\left(2\lambda\sqrt{1+kt}\right)}$. The quenched averaged violation can be expressed as

$$\langle \mathcal{Q} \rangle^O = \frac{2}{\sigma_\lambda \sqrt{2\pi}} \times \int_{-\infty}^{\infty} \exp\frac{(\lambda - \bar{\lambda})^2}{2\sigma_\lambda^2} \sqrt{1 + \sin^2(2\lambda\sqrt{1 + kt})} d\lambda. \quad (45)$$

Since there is no closed form expression of this integral, we resort to standard numerical techniques to perform this integration. As an example, we choose three sets of system parameters, k=0,4,8, where $\langle\lambda\rangle=1.0$, and $\sigma_\lambda=0.1$ and

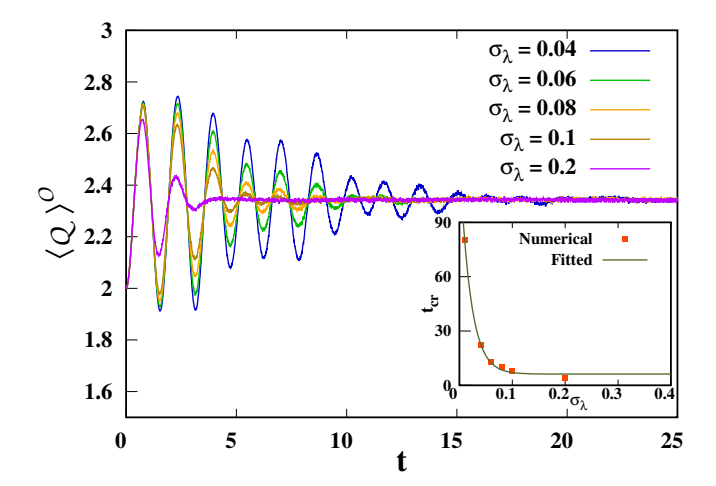


FIG. 11. (Color online.) Dynamics of $\langle \mathcal{Q} \rangle^O$ (ordinate) vs t (abscissa). The initial CV part of the hybrid system is in a coherent state with $|\alpha|=0.2$ and mean interaction strength is $\bar{\lambda}=1.0$. We take different values of standard deviation in λ denoted by $\sigma_{\lambda}=0.04,0.06,0.08,0.1$ and 0.2. (Inset) The critical time, t_{cr} (vertical axis), i.e., the time when $\langle \mathcal{Q} \rangle^O$ reaches the saturation value $\langle \mathcal{Q} \rangle^O_{\rm sat}$ against strength of the disorder, σ_{λ} (horizontal axis). The number of realizations considered to perform quenched averaging is 7000. All the axes are dimensionless.

plot their corresponding $\langle \mathcal{Q} \rangle^O$ for various times. In each of the cases, we observe the following:

- (1) The quenched averaged maximal violation after some initial oscillations saturate. Irrespective of k values, we, interestingly, find that the quenched averaged violation, $\langle \mathcal{Q} \rangle^O$, saturates to ≈ 2.43 , see Fig. 10. The fact that the measurement settings can be tuned based on the particular disorder realization λ generates an atypical consequence. The saturated quenched averaged violation of Bell inequality $\langle \mathcal{Q} \rangle_{\rm sat}^O \approx 2.43$ remains invariant under different disorder strengths, σ_{λ} .
- (2) Relative saturation times for different k values have same pattern. In particular, we see that for higher k values, the saturation times, t_{cr} are shorter than the one obtained with low k. This might be interpreted from the fact that the integrand in Eq. (45) oscillates with a higher frequency for large k values compared to the one with low k values. The integration results in the cancellation of these fast oscillating terms, thereby leading to a quicker saturation for larger k values.
- (3) In addition, our investigation also reveals that the saturation times can be shorten with the increase of $\bar{\lambda}$ and σ_{λ} .

We carry out a similar analysis for other choices of the initial state. An initial product state with the field state being in the coherent state and the atom being in the excited state, see Eq.[28]. Note that all the other choices of initial states considered in this manuscript produce qualitatively similar results. Nevertheless, here also, the time dynamics of the quenched averaged maximal violation of Bell inequality observe a similar trend to when the initial state was taken to be in any of the Fock states – initial oscillations followed by saturation, as depicted in Fig. 11 for various choice of disorder parameters. However, unlike in the previous case where the saturated value of the quenched averaged maximal violation is independent of

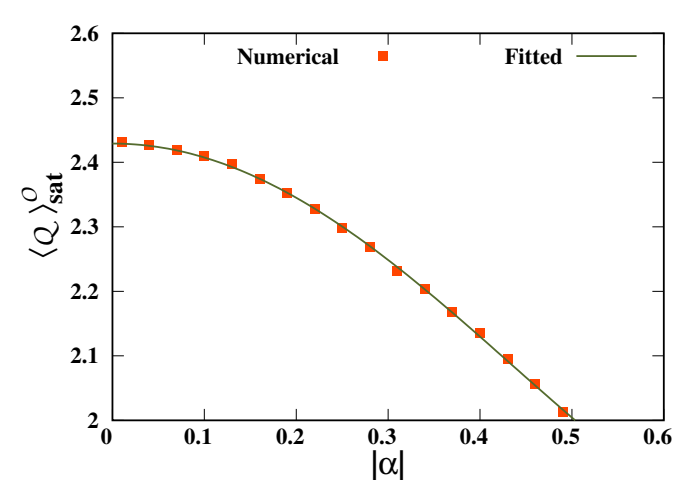


FIG. 12. (Color online.) The saturation value of the quenched averaged violation of Bell inequality, $\langle \mathcal{Q} \rangle_{\mathrm{sat}}^O$ (ordinate) with oracle measurement strategy against displacement of coherent state of the initial hybrid state, $|\alpha|$ (abscissa). $\langle \mathcal{Q} \rangle_{\mathrm{sat}}^O$ decreases with $|\alpha|$ till some critical value $|\alpha|_{cr}=0.51$ beyond which the violation vanishes. Both axes are dimensionless.

k, here the saturated value $\langle \mathcal{Q} \rangle_{\mathrm{sat}}^O$ decreases with the increase of $|\alpha|$, see Fig. 12. In particular, we find a critical value of $|\alpha| = |\alpha_{cr}| \approx 0.51$ such that $\langle \mathcal{Q} \rangle_{\mathrm{sat}}^O = 0$, for $|\alpha| > |\alpha_{cr}|$. By employing the χ -square curve fitting, we realize that the functional form of $\langle \mathcal{Q} \rangle_{\mathrm{sat}}^O$ with $|\alpha|$ to be $a + b|\alpha|^2 + c|\alpha|^4$ with a = 2.43, b = -2.18 and c = 1.91 having maximum 1.92% errors in parameters, as shown in Fig. 12.

We also investigate how the critical time t_{cr} for $\langle \mathcal{Q} \rangle^O$ to saturate, varies with the disorder parameters and find it to be decreasing with increasing σ_{λ} before eventually saturating at a constant value (see Fig. 11). Further by using the χ -square curve fitting, the functional form of t_{cr} with σ_{λ} is found to be $b+c\exp(-d(\sigma_{\lambda}-0.01))$ with b=6.20, c=73.40 and d=49.30 having maximum 10.0% errors in parameters. Interestingly, like in the previous case where the initial CV state was taken to be in a Fock state, the saturated quenched averaged violation of Bell inequality is independent of the disorder strength σ_{λ} .

B. Realistic measurement strategy

In the previous situation, we assumed that the experimentalist can adjust the measurement settings depending on the particular realization of the disorder. In a more realistic scenario, the experimentalist has information only about some global properties of the disorder, say a few moments or the range of the distribution. For example, if the disorder is Gaussian, the measurement strategy is fixed only on the knowledge of the mean $\bar{\lambda}$ and the standard deviation σ_{λ} . One reasonable strategy that one can employ is to fix the measurement settings that are optimal for the mean of the disorder distribution $\bar{\lambda}$ for all cases. This choice is irrespective of the standard deviation σ_{λ} . In absence of realization-dependent tuning of measurement settings, this strategy seems to be the only rational one

and, therefore, we consider this for our investigation.

We now compute the quenched averaged violation of local realism when the measurement settings are fixed to the direction that is optimal for the mean value $\bar{\lambda}$ of the disorder. For this, we first rewrite Eq. (42) in a form to explicitly illustrate how the measurement settings enter the Bell expression as

$$Q^{O}(\lambda) = \sqrt{||T_{\lambda}.C_{\lambda}||^{2} + ||T_{\lambda}.C_{\lambda}'||^{2}},$$
(46)

where C_{λ} and C'_{λ} are two eigenvectors of T_{λ} corresponding to the two largest eigenvalues in \mathbb{R}_3 . The norm of a vector X is given by $||X|| = \sqrt{X^{\dagger}X}$. Physically, C_{λ} and C'_{λ} come from the tuning the measurement direction optimally for a given realization λ , and hence denote the measurement settings. When the measurement direction is fixed to the one which is optimal for $\bar{\lambda}$, for a given realization λ , we get

$$Q^{P}(\lambda) = \sqrt{||T_{\lambda}.C_{\bar{\lambda}}||^{2} + ||T_{\lambda}.C_{\bar{\lambda}}'||^{2}}.$$
 (47)

Similar to the previous section, we take the quenched averaged value over different realizations is given by $\langle \mathcal{Q} \rangle^P = \int \mathcal{Q}^P(\lambda) P(\lambda) d\lambda$. Note that we clearly have $\mathcal{Q}^P(\lambda) \leq \mathcal{Q}^O(\lambda)$ which directly translates to $\langle \mathcal{Q} \rangle^P \leq \langle \mathcal{Q} \rangle^O$. The equality holds when $P(\lambda) = \delta(\lambda - \bar{\lambda})$.

Realistic measurement scenario captures truly the essence of stochasticity in the system parameters and shows a drastically different dynamics with time. In the previous scenario, we found a saturation time of $\langle \mathcal{Q} \rangle^O$. In this realistic scenario, as the measurement settings is fixed to give maximal violation for λ , for realizations that are more deviated from λ will contribute more non-optimally towards the quenched averaged value. For this reason, we are unable to find a situation where $\langle \mathcal{Q} \rangle^P > 2$ through the whole time. We observe that the violation $\langle \mathcal{Q} \rangle^P$ obtained for disordered situation is enveloped by the violation of Bell inequality by the ordered system ($\sigma_{\lambda} = 0$). Moreover, for any value of $\sigma_{\lambda} > 0$, we find that $\langle \mathcal{Q} \rangle^P$ oscillates until a critical time t_{cr} , such that for $t > t_{cr}$, the value of $\langle \mathcal{Q} \rangle^P$ goes below 2. Hence, the realistic measurement settings with stochastic evolution parameter can only catch the violation of local realism up to a certain time t_{cr} for a given σ_{λ} (as depicted in Fig. 13).

VI. CONCLUSION

The detection of nonlocality and nonclassicalaity in continuous variable (CV) quantum systems has received a great deal of attention with the advancement of photonic quantum information technologies. On the other hand, in discrete systems, violations of local realism have been thoroughly studied over the years as a component of experimentally viable entanglement detection criteria and as a means of addressing the fundamental question of the completeness of quantum mechanics posed by Einstein-Podolosky and Rosen. Like violation of Bell inequalities, negative Wigner volume corresponding to quantum systems indicates correlations present in the quantum systems which cannot be classically simulated, although

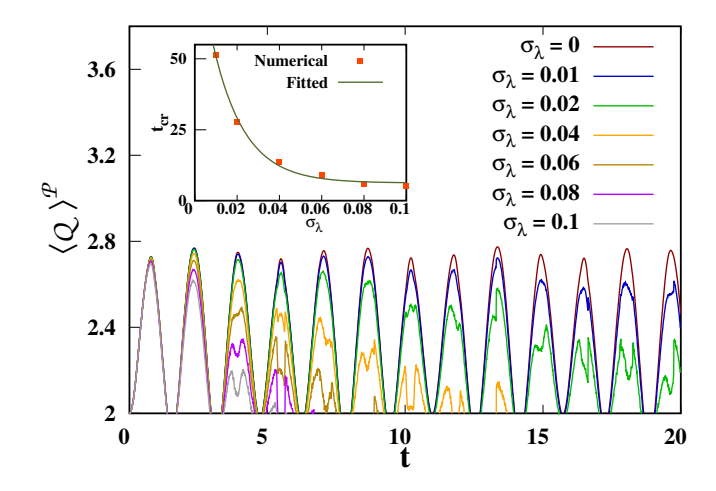


FIG. 13. (Color online.) Comparing the quenched averaged value of the violation of Bell inequalities $\langle \mathcal{Q} \rangle^P$ (ordinate) with time t (abscissa) in realistic measurement settings for 7000 realizations. (Inset) The critical time t_{cr} (ordinate) until which it is capable of detecting a violation of Bell inequality after quenched averaging vs σ_{λ} (abscissa). The initial state of the mode is taken to be in a coherent state with $|\alpha|=0.2$. Further, by using the χ -square curve fitting, we find the functional form of t_{cr} with σ_{λ} to be $b+c\exp(-d(\sigma_{\lambda}-0.01))$ (b=6.24, c=44.65 and d=66.79 having maximum 10.0% errors in parameters). All the axes are dimensionless.

there is no strong connection between negative Wigner volume and violation of Bell inequalities. In this work, we exploited hybrid measurements made up of spin and pseudospin measurements to compute Bell correlations for detecting entanglement in hybrid systems composed of both discrete and CV systems.

We investigated the maximal violation of Bell inequalities and Wigner negativity in the dynamics of the hybrid system produced by the Jaynes-Cummings interaction between finite- and the infinite-dimensional CV systems. In particular, starting with the product, classically correlated, and entangled states, we investigated the pattern in the violation of Bell inequalities of the evolved state and discovered how the violation depends on the system characteristics, notably those involved in CV systems. We found that the violation of Bell inequalities based on hybrid measurements is sufficient but not necessary by analyzing the entanglement features of the dynamical states.

Deviating from the ideal scenario, we assumed that the interaction strength between the CV and the discrete systems has a fluctuation around a mean value. Following the oracle measurement strategy in which the measurement settings in the Bell expression can be tuned depending on the realization of a particular choice of a parameter, we demonstrated that the quenched averaged value of the maximal violation of the Bell inequality saturates with time to a particular value, independent of the fluctuation strength of the interaction parameter and with the moderate values of the displacement strength in the coherent state. However, in the ordered case, it is always oscillating with time. Therefore, the clear advantage of the disordered systems over the ordered case emerges in

presence of moderate displacement value where the saturated value is finite for the entire time duration after the initial oscillation although the evolved state does not show violation with the increase of the displacement parameter. Moreover, we presented a more realistic measurement strategy where the measurement direction is fixed to the direction of the maximal violation of Bell inequality for the mean value of interaction strength. In this case, the violation of Bell inequality in the dynamical state does not saturate to a particular value – the violation decreases with time, which depends primarily on the standard deviation of the interaction strength, and it finally vanishes. The formalism presented in this work paves the way to demonstrate the nonlocality in hybrid quantum systems, thereby providing a device independent detection method of entanglement in laboratories.

ACKNWOLEDGEMENTS

We thank Ganesh for fruitful discussions. PH, RB, and ASD acknowledge the support from the Interdisciplinary

Cyber Physical Systems (ICPS) program of the Department of Science and Technology (DST), India, Grant No.: DST/ICPS/QuST/Theme- 1/2019/23. This research was supported in part by the 'INFOSYS scholarship for senior students'. We acknowledge the use of QIClib – a modern C++ library for general purpose quantum information processing and quantum computing (https://titaschanda.github.io/QIClib), and the cluster computing facility at the Harish-Chandra Research Institute. This work has been partly supported by the Hong Kong Research Grant Council (RGC) through grant 17300918.

- [1] J. S. Bell, Physics Physique Fizika 1, 195 (1964).
- [2] A. Einstein, B. Podolsky, and N. Rosen, Phys. Rev. 47, 777 (1935).
- [3] S. J. Freedman and J. F. Clauser, Phys. Rev. Lett. 28, 938 (1972).
- [4] A. Aspect, P. Grangier, and G. Roger, Phys. Rev. Lett. 47, 460 (1981).
- [5] A. Aspect, P. Grangier, and G. Roger, Phys. Rev. Lett. 49, 91 (1982).
- [6] B. Hensen, H. Bernien, A. E. Dréau, A. Reiserer, N. Kalb, M. S. Blok, J. Ruitenberg, R. F. L. Vermeulen, R. N. Schouten, C. Abellán, W. Amaya, V. Pruneri, M. W. Mitchell, M. Markham, D. J. Twitchen, D. Elkouss, S. Wehner, T. H. Taminiau, and R. Hanson, Nature 526, 682 (2015).
- [7] W. Zhang, T. van Leent, K. Redeker, R. Garthoff, R. Schwonnek, F. Fertig, S. Eppelt, W. Rosenfeld, V. Scarani, C. C.-W. Lim, and H. Weinfurter, Nature 607, 687 (2022).
- [8] D. P. Nadlinger, P. Drmota, B. C. Nichol, G. Araneda, D. Main, R. Srinivas, D. M. Lucas, C. J. Ballance, K. Ivanov, E. Y.-Z. Tan, P. Sekatski, R. L. Urbanke, R. Renner, N. Sangouard, and J.-D. Bancal, Nature 607, 682 (2022).
- [9] Y. Liu, Q. Zhao, M.-H. Li, J.-Y. Guan, Y. Zhang, B. Bai, W. Zhang, W.-Z. Liu, C. Wu, X. Yuan, H. Li, W. J. Munro, Z. Wang, L. You, J. Zhang, X. Ma, J. Fan, Q. Zhang, and J.-W. Pan, Nature 562, 548 (2018).
- [10] I. Šupić and J. Bowles, Quantum 4, 337 (2020).
- [11] N. Brunner, D. Cavalcanti, S. Pironio, V. Scarani, and S. Wehner, Rev. Mod. Phys. 86, 419 (2014).
- [12] E. Chitambar and G. Gour, Rev. Mod. Phys. 91, 025001 (2019).
- [13] G. Kurizki, P. Bertet, Y. Kubo, K. Mølmer, D. Petrosyan, P. Rabl, and J. Schmiedmayer, Proceedings of the National Academy of Sciences 112, 3866 (2015).
- [14] U. L. Andersen, J. S. Neergaard-Nielsen, P. van Loock, and A. Furusawa, Nature Physics 11, 713 (2015).
- [15] E. Agudelo, J. Sperling, L. S. Costanzo, M. Bellini, A. Zavatta, and W. Vogel, Phys. Rev. Lett. 119, 120403 (2017).

- [16] K. Kreis and P. van Loock, Phys. Rev. A 85, 032307 (2012).
- [17] H. Jeong, A. Zavatta, M. Kang, S.-W. Lee, L. S. Costanzo, S. Grandi, T. C. Ralph, and M. Bellini, Nature Photonics 8, 564 (2014).
- [18] I. I. Arkhipov, A. Barasiński, and J. Svozilík, Scientific Reports **8** (2018), 10.1038/s41598-018-35330-6.
- [19] K. Banaszek and K. Wódkiewicz, Phys. Rev. A 58, 4345 (1998).
- [20] Z.-B. Chen, J.-W. Pan, G. Hou, and Y.-D. Zhang, Phys. Rev. Lett. 88, 040406 (2002).
- [21] B. Zhang, Z.-R. Zhong, and S.-B. Zheng, Physics Letters A 375, 1765 (2011).
- [22] S. Roy, T. Chanda, T. Das, A. Sen(De), and U. Sen, Phys. Rev. A 98, 052131 (2018).
- [23] E. Jaynes and F. Cummings, Proceedings of the IEEE **51**, 89 (1963).
- [24] C. Gerry and P. Knight, *Introductory Quantum Optics* (Cambridge University Press, 2004).
- [25] A. Kenfack and K. yczkowski, Journal of Optics B: Quantum and Semiclassical Optics 6, 396 (2004).
- [26] J. F. Clauser, M. A. Horne, A. Shimony, and R. A. Holt, Phys. Rev. Lett. 23, 880 (1969).
- [27] J. F. Clauser, M. A. Horne, A. Shimony, and R. A. Holt, Phys. Rev. Lett. 24, 549 (1970).
- [28] A. Fine, Phys. Rev. Lett. 48, 291 (1982).
- [29] B. S. Cirel'son, Letters in Mathematical Physics 4, 93 (1980).
- [30] R. Horodecki, P. Horodecki, and M. Horodecki, Physics Letters A 200, 340 (1995).
- [31] E. Wigner, Phys. Rev. 40, 749 (1932).
- [32] G. Adesso, S. Ragy, and A. R. Lee, Open Systems & Information Dynamics 21, 1440001 (2014), https://doi.org/10.1142/S1230161214400010.
- [33] T. Tilma, M. J. Everitt, J. H. Samson, W. J. Munro, and K. Nemoto, Phys. Rev. Lett. 117, 180401 (2016).
- [34] I. Bengtsson and K. Zyczkowski, Geometry of Quantum States: An Introduction to Quantum Entanglement (Cambridge Univer-

- sity Press, 2006).
- [35] K. Jürgens, F. Lengers, D. Groll, D. E. Reiter, D. Wigger, and T. Kuhn, Phys. Rev. B 104, 205308 (2021).
- [36] C. Savage, Journal of Modern Optics 37, 1711 (1990), https://doi.org/10.1080/09500349014551941.
- [37] A. Blais, S. M. Girvin, and W. D. Oliver, Nature Physics 3, 247 (2020).
- [38] P. Meystre, Physics Reports **219**, 243 (1992).
- [39] A. Ghoshal, S. Das, A. Sen(De), and U. Sen, Phys. Rev. A 101, 053805 (2020).
- [40] J. Billy, V. Josse, Z. Zuo, A. Bernard, B. Hambrecht, P. Lugan, D. Clément, L. Sanchez-Palencia, P. Bouyer, and A. Aspect, Nature 453, 891 (2008).
- [41] G. Roati, C. D'Errico, L. Fallani, M. Fattori, C. Fort, M. Zaccanti, G. Modugno, M. Modugno, and M. Inguscio, Nature 453, 895 (2008).

- [42] M. Lewenstein, A. Sanpera, V. Ahufinger, B. Damski, A. Sen(De), and U. Sen, Advances in Physics 56, 243 (2007), https://doi.org/10.1080/00018730701223200.
- [43] A. Aspect and M. Inguscio, Physics Today 62, 30 (2009), https://doi.org/10.1063/1.3206092.
- [44] S. Sachdev, *Quantum Phase Transitions*, 2nd ed. (Cambridge University Press, 2011).
- [45] H. Nishimori, Statistical Physics of Spin Glasses and Information Processing An Introduction (Clarendon Press, 2001).
- [46] D. Chowdhury, *Spin Glasses and Other Frustrated Systems* (World Scientific Publishing, 1986).
- [47] S. Suzuki, J.-I. Inoue, and B. K. Chakrabarti, *Quantum Ising Phases and Transitions in Transverse Ising Models*, Vol. 859 (2013).
- [48] B. K. Chakrabarti, A. Dutta, and P. Sen, *Quantum Ising Phases and Transitions in Transverse Ising Models* (Springer, 1986).
- [49] R. Horodecki, P. Horodecki, M. Horodecki, and K. Horodecki, Rev. Mod. Phys. 81, 865 (2009).